Materials Today Bio 17 (2022) 100496

Contents lists available at ScienceDirect

Materials Today Bio

journal homepage: www.journals.elsevier.com/materials-today-bio

Spongy-like hydrogels prevascularization with the adipose tissue vascular fraction delays cutaneous wound healing by sustaining inflammatory cell influx

Helena R. Moreira [a,b], Daniel B. Rodrigues [a,b], Sara Freitas-Ribeiro [a,b], Lucília P. da Silva [a,b], Alain da S. Morais [a,b], Mariana Jarnalo [c,d], Ricardo Horta [c,d], Rui L. Reis [a,b], Rogério P. Pirraco [a,b], Alexandra P. Marques [a,b,*]

[a] 3B's Research Group, I3Bs – Research Institute on Biomaterials, Biodegradables and Biomimetics, University of Minho, Headquarters of the European Institute of Excellence on Tissue Engineering and Regenerative Medicine, Avepark – Zona Industrial da Gandra, Guimaraes, 4805-017, Portugal
[b] ICVS/3B's – PT Government Associate Laboratory, Braga/Guimaraes, 4805-017, Portugal
[c] Department of Plastic and Reconstructive Surgery, And Burn Unity, Centro Hospitalar de São João, Porto, Portugal
[d] Faculty of Medicine - University of Porto, Portugal

ARTICLE INFO

Keywords:
Integrin-specific biomaterials
Stromal vascular fraction
Wound healing
Re-epithelization
Inflammation
Remodeling

ABSTRACT

In vitro prevascularization is one of the most explored approaches to foster engineered tissue vascularization. We previously demonstrated a benefit in tissue neovascularization by using integrin-specific biomaterials prevascularized by stromal vascular fraction (SVF) cells, which triggered vasculogenesis in the absence of extrinsic growth factors. SVF cells are also associated to biological processes important in cutaneous wound healing. Thus, we aimed to investigate whether in vitro construct prevascularization with SVF accelerates the healing cascade by fostering early vascularization vis-à-vis SVF seeding prior to implantation. Prevascularized constructs delayed re-epithelization of full-thickness mice wounds compared to both non-prevascularized and control (no SVF) groups. Our results suggest this delay is due to a persistent inflammation as indicated by a significantly lower M2($CD163^+$)/M1($CD86^+$) macrophage subtype ratio. Moreover, a slower transition from the inflammatory to the proliferative phase of the healing was confirmed by reduced extracellular matrix deposition and increased presence of thick collagen fibers from early time-points, suggesting the prevalence of fiber crosslinking in relation to neodeposition. Overall, while prevascularization potentiates inflammatory cell influx, which negatively impacts the cutaneous wound healing cascade, an effective wound healing was guaranteed in non-prevascularized SVF cell-containing spongy-like hydrogels confirming that the SVF can have enhanced efficacy.

1. Introduction

In cutaneous wounds, neovascularization is critical for tissue repair. From the early onset of the healing cascade, capillaries sprout from the host vasculature invading the fibrin clot and vascularizing the granulation tissue [1]. This pro-angiogenic phase is critical to provide nutrients and oxygen to a metabolically active wound bed and is directly associated to an immature capillary network that also potentiates extravasation of inflammatory cells into the wound bed. In turn, a healthy vascularized granulation tissue provides the support for the growth and migration of keratinocytes that start the re-epithelialization of the wound. As the healing progresses and the inflammation is resolved, the dense neovascular network matures experiencing a significant regression regulated by antiangiogenic stimuli. It is then understandable that given all this interplay among the different stages/processes, any alteration in the angiogenic signaling - e.g., reduced production of pro-angiogenic cytokines, overproduction of anti-angiogenic cytokines, overgranulation - may compromise the whole process impairing healing and skin repair [2].

The strategies used to promote neovascularization in cutaneous wounds have been mainly focusing on the in situ controlled delivery of angiogenic growth factors [3–6] or respective encoding genetic material

* Corresponding author. 3B's Research Group, I3Bs – Research Institute on Biomaterials, Biodegradables and Biomimetics, University of Minho, Headquarters of the European Institute of Excellence on Tissue Engineering and Regenerative Medicine, Avepark – Zona Industrial da Gandra, Guimaraes, 4805-017, Portugal.
E-mail address: apmarques@i3bs.uminho.pt (A.P. Marques).

https://doi.org/10.1016/j.mtbio.2022.100496
Received 28 July 2022; Received in revised form 3 November 2022; Accepted 13 November 2022
Available online 14 November 2022

[7,8], transplantation of adult stem cells [9–13] or, on the implantation of prevascularized constructs using both mature [14,15] and progenitor [16,17] endothelial cells. Despite the significant achievements, all these strategies have issues that are still far from being resolved and have been hampering its clinical translation. While growth factors sustained temporal delivery is possible, it is also often associated to bolus release and unmatched profile with the wound requirements. Short half-life due to lack of protection from proteolytic degradation, and high doses to achieve a therapeutic effect [18] are also shortcomings that might be tackled by the in situ secretion of growth factors by genetically modified cells. Yet, reduced transfection efficiency, and immunogenicity issues and potential long-term side effects are still associated to these strategies. In vitro prevascularization is one of the most successful approaches in fostering vascularization at wound site. However, the clinical use of those angiogenic cells is highly hampered by an insufficient number required for therapy due to highly difficult isolation procedures and limited expansion in vitro [19]. Other cellular approaches with less manipulation have been showing a positive impact in the vascularization of cutaneous wounds mostly provided by an angiogenic secretome, such as the case of adipose derived stem cells (hASCs) [20–22]. Yet, their potential might still be maximized by enhancing their residence time at the wound site.

Interestingly, several works have also suggested an impact of ASCs in cutaneous wounds that goes beyond neovascularization including a paracrine interaction with the resident cells that affects epidermal morphogenesis [9,23], and regulates inflammation [24,25]. Moreover, clinical trials with the stromal vascular fraction (SVF) of the adipose tissue, which comprises cells subpopulations other than the ASCs [26,27] showed that 93% of the patients with chronic non-healing diabetic foot ulcers achieved full closure - the remaining had a wound closure >85% - after autologous SVF transplantation [28]. Comparable outcomes were attained with SVF incorporated in a fibrin-collagen hydrogel confirming a faster re-epithelialization in the presence of SVF [29]. While the mechanism of action is yet to be determined, pre-clinical studies revealed a faster progression in the healing of full-thickness wounds treated with SVF characterized by earlier resolution of the inflammatory phase accompanied by fibroblasts proliferation [30].

In our previous work we demonstrated a benefit in tissue neovascularization with integrin-specific biomaterials pre-vascularized by SVF cells capable of triggering vasculogenesis in the absence of extrinsic growth factors [31]. Herein, we hypothesized that an in vitro prevascularization stage would accelerate the healing cascade by fostering the early vascularization of the wound by inosculating with the host vasculature, further potentiating the effect of SVF. To validate this, we assessed the capacity of prevascularized and non-prevascularized - containing freshly isolated SVF cells - constructs to modulate wound inflammation and re-epithelization, and neotissue deposition and remodeling (Fig. 1).

2. Results

2.1. Popularization of the constructs by SVF cells

Besides endothelial progenitor and mature cells which highly express the αvβ3 integrin [32,33] and are the ones responsible for the prevascularization of the constructs, SVF contains a multitude of other cells (Fig. 2a). Overall, SVF cells were entrapped in the spongy-like hydrogels after seeding. However, a significant ($p < 0.05$) reduction (about 50%) in the number of cells was observed from day 0 to day 3 of culture (Fig. 2b). At this timepoint, most of the remnant cells were alive (Fig. 2c) although they did not seem to proliferate with increasing culture time (Fig. 2b). When we looked at the phenotype of the cells entrapped in the spongy-like hydrogels, we confirmed that at day 0 SVF cells displayed the typically characteristics [27] linked to the mesenchymal (CD105, CD73, CD90), pericytic (CD146), mature/progenitor endothelial (CD31, CD34, CD105) and hematopoietic (CD45) phenotype (Fig. 2d, i). Along the culture, a significant ($p < 0.05$) decrease was noticed regarding the percentage of positive cells expressing CD73 and CD90 markers while the opposite trend was observed for CD31 and CD105 demonstrating a preferred retention of angiogenic/vasculogenic cells in the spongy-like hydrogels. Interestingly, these cells seem to be supported along time by other adherent cells ($CD31^-$) to organize in capillary-like structures (Fig. 2d, ii). After 7 days of culture a pre-vascularized construct with these structures lined by basement membrane proteins such as laminin, fibronectin and collagen type IV was attained (Fig. 2e).

2.2. Wound healing progression

In order to confirm that the pre-vascularization of the construct had a positive impact in the overall wound healing cascade, we analyzed the different stages in comparison with the non-prevascularized conditions - freshly isolated SVF was seeded in the material and immediately implanted (SVFnpv) (Fig. 3a).

2.2.1. Wound closure and neoepidermis structure

Upon implantation, although complete wound closure was reached at day 28 in all group (Fig. 3b), there seems to be a tendency of slower wound closure rate for the prevascularized group. Indeed, the wound closure percentage at day 11 in this condition was significantly lower ($p < 0.05$) than in the other groups (Fig. 3b). This delayed re-

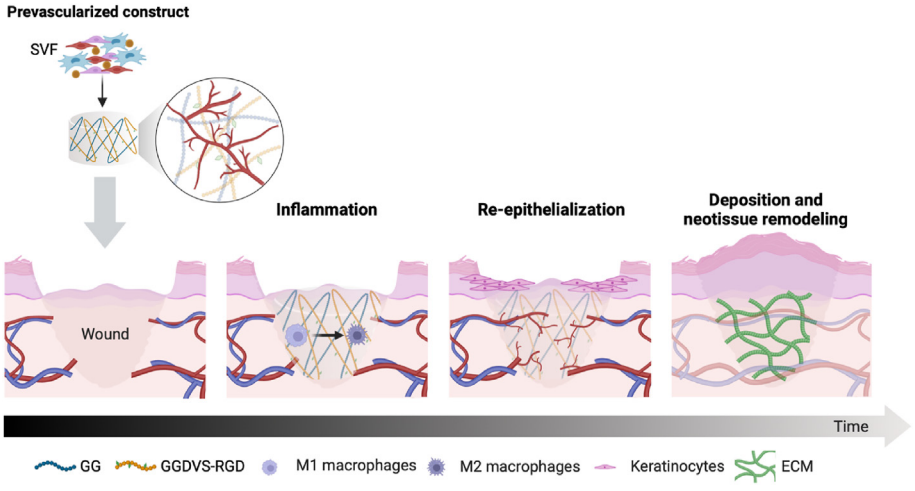

Fig. 1. Schematic representation of the rationale. Vasculogenic cells present in the stromal vascular fraction (SVF) of adipose tissue are retained in the integrin-specific gellan gum (GG) spongy-like hydrogels prevascularizing the construct in the absence of extrinsic growth factors. The prevascular network will inosculate with the host vasculature accelerating the healing cascade fostering the resolution of the inflammation and the re-epithelialization of the wound which then impacts extracellular matrix (ECM) deposition and neotissue remodeling.

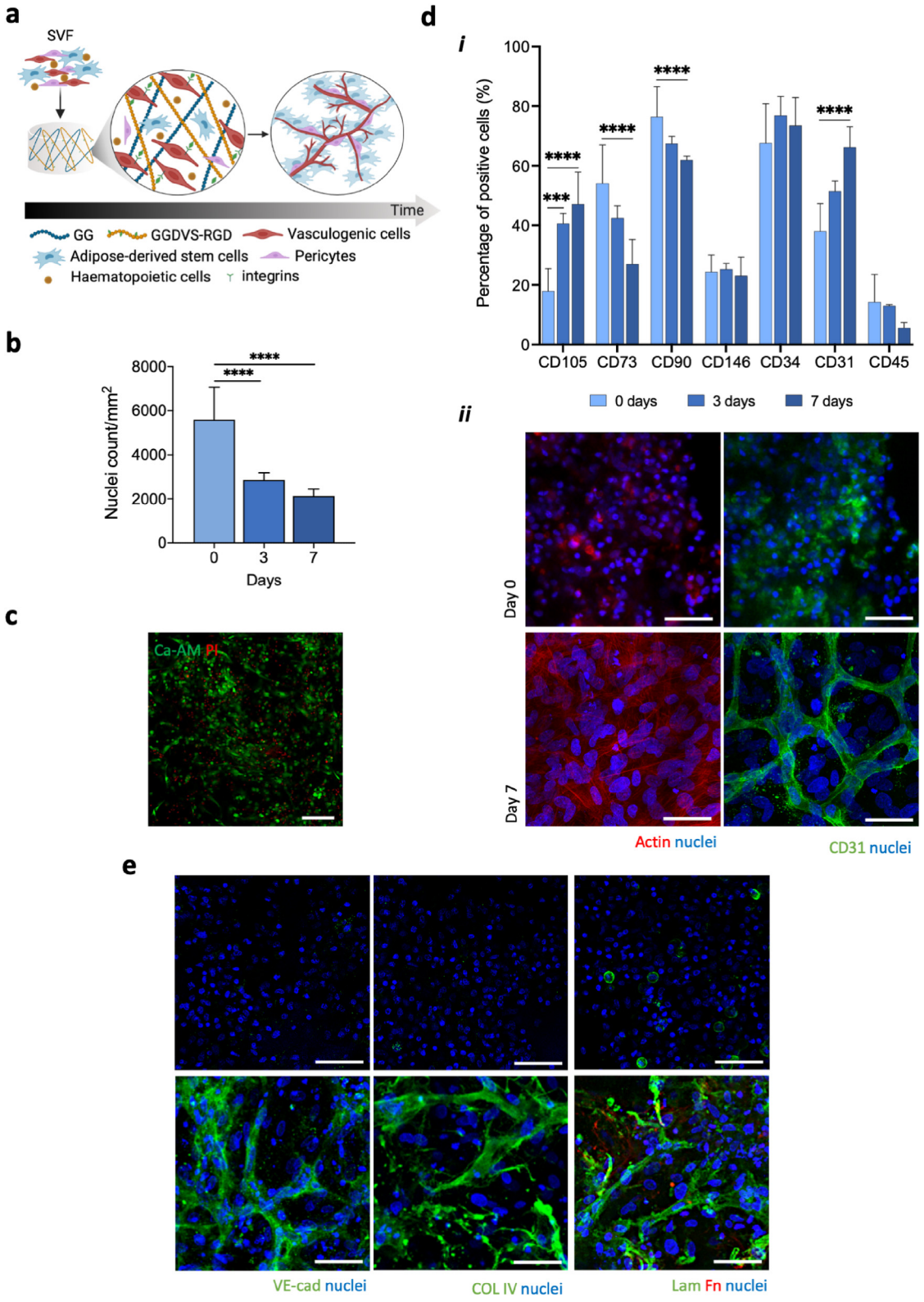

Fig. 2. Performance of SVF cells in the integrin-specific gellan gum (GG) spongy-like hydrogels. a Schematic representation of the different cell subpopulations present in the stromal vascular fraction (SVF) of adipose tissue and how they organize within the spongy-like hydrogel along the culture. **b** Total number of SVF cells entrapped in the materials after seeding (day 0) and 3 and 7 days of culture. **c** Survival of SVF cells after 3 days in culture determined after calcein AM (Ca-AM, live, green) and propidium iodide (PI, dead, red) staining. Scale bar = 500 μm **d** (i) Expression profile of membrane markers by SVF cells after seeding (day 0) and 3 and 7 days of culture determined by flow cytometry. (ii) Representative images of the F-actin cytoskeleton and expression of CD31 after seeding (day 0) and 7 days of culture. Scale bar = 50 μm **e** Representative immunocytochemistry images of the expression of VE-cadherin (VE-cad), Collagen type IV (COL IV), Laminin (Lam), Fibronectin (Fn) after seeding (0 days) and 7 days of culture. Nuclei were counterstained with DAPI (nuclei). Scale bar = 50 μm. Quantitative results are expressed as the mean ± standard deviation where n = 3, *$p < 0.05$, ***$p < 0.001$, ****$p < 0.0001$, one-way ANOVA with Tukey multiple comparison post-test.

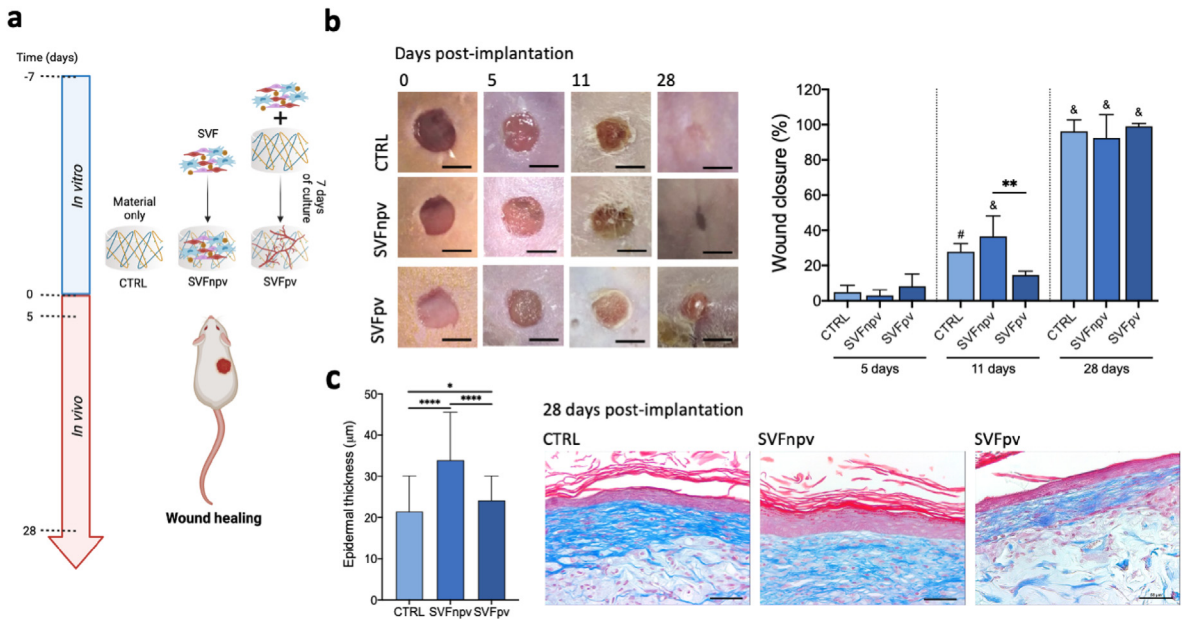

Fig. 3. Impact in the re-epithelialization. a Schematic representation of the test groups: CTRL (GG/GGDVS-RGD spongy-like hydrogels without cells), SVFnpv (freshly isolated SVF seeded in the material), SVFpv (SVF seeded in the material and cultured for 7 days in vitro prior to implantation). **b** Representative macroscopic images of the wounds and representation of the percentage of wound closure up to 28 days of implantation. Scale bar = 5 mm **c** Quantification of the epidermal thickness and representative images of Masson's Trichrome (MT) staining at day 28 detailing the neoepidermis features. Scale bar = 50 μm. Quantitative results are expressed as the mean ± standard deviation where n = 3, *$p < 0.05$, **, #$p < 0.01$, ***$p < 0.001$, ****, &$p < 0.0001$, one-way or two-way ANOVA with Tukey multiple comparison post-test. #, & refers to the significance difference of the same group related to day 5.

epithelialization led to a significantly ($p < 0.05$) thinner neoepidermis consisting of 2–3 layers of keratinocytes in the prevascularized group, similar to the control at day 28 post-implantation (Fig. 3c). Interestingly, the neoepidermis in the prevascularized groups was also characterized by the absence or the presence of a very thin stratum corneum, in opposition to the prominent layer observed in the non-prevascularized condition, which was akin to the control.

2.2.2. *Inflammatory response*

Neovascularization cannot be dissociated from the inflammatory response since vascular hyperpermeability allows inflammatory mediators and immune cells to infiltrate the injured site [34]. In cutaneous wounds, persistent inflammation and compromised transition to the proliferative phase is linked to delayed and even pathological healing [35,36]. Therefore, we wanted to understand how prevascularization correlates with the progression of the healing of the wound. Integrin-specific biomaterials were well integrated in the wound site and infiltrated with an inflammatory exudate 5 days after implantation independently of the group (Fig. 4a). At day 28 post-implantation, this inflammatory exudate was only observed in the prevascularized group (Fig. 4a, i-iii), which can be associated to the presence of the transplanted material, which was barely detected in the non-prevascularized and control groups.

The analysis of the inflammatory infiltrate at day 5 showed a significantly ($p < 0.05$) higher percentage of M1-polarized ($CD86^+$) macrophages in the prevascularized group (Fig. 4b). In turn, the percentage of M2-polarized ($CD163^+$) macrophages in both experimental conditions (SVFnpv and SVFpv) was significantly ($p < 0.05$) higher than in the control. With time, the percentage of $CD86^+$ macrophages decreased for all the conditions but the differences among the groups remained. On the other hand, the percentage of $CD163^+$ macrophages at day 28 post-transplantation was lower in the prevascularized condition while decreasing in the SVFpv group and increasing in the control. These variations resulted in a $CD163^+/CD86^+$ ratio similar for SVFnpv and control conditions but significantly ($p < 0.05$) lower for the SVFpv group, suggesting a persistence in the inflammatory stage of the wound healing for this group.

2.2.3. *ECM deposition*

Based on the persistent inflammation results from the prevascularised constructs, we further analyzed the deposition of new extracellular matrix to confirm the status of the healing process. As expected at the early time-point, no differences were observed among the different conditions regarding the deposited collagen (Fig. 5a and b). At day 28 post-implantation, the abundance of collagen was significantly ($p < 0.05$) lower in the SVFpv condition than in the SVFnpv and control ones (Fig. 5a and b). In the SVFpv condition, the collagen fibers were randomly distributed mostly within the construct structure, whereas in the SVFnpvand control groups those fibers were more organized and located both within and in the surroundings of the structure (Fig. 5a i-iii). Interestingly, in the SVFpv group collagen was mostly organized as thick fibers as from early time-points (Fig. 6a and b, Supplementary Fig. 1) suggesting the prevalence of fibers crosslinking in relation to neo-deposition. In opposition, the abundance of thin collagen fibers at the latter timepoint was significantly higher in the SVFnpv and control groups than in the SVFpv, while the amount of thick fibers was residual (Supplementary Fig. 1). This suggests a reduced fibroblast's activity in the prevascularized condition, characteristic of the proliferative wound healing stage.

3. Discussion

Neovascularization is a critical step in the wound healing cascade being therefore determinant for a successful outcome. While different strategies have been used to tackle neovascularization at the wound site, pre-vascularization is one of the most effective. However, its clinical translation has been highly hampered by an insufficient number required for therapy. We previously shown that SVF cells respond to integrin-specific 3D matrices triggering vasculogenesis in vitro in the absence of extrinsic growth factors [31]. Moreover, we provided evidence that this

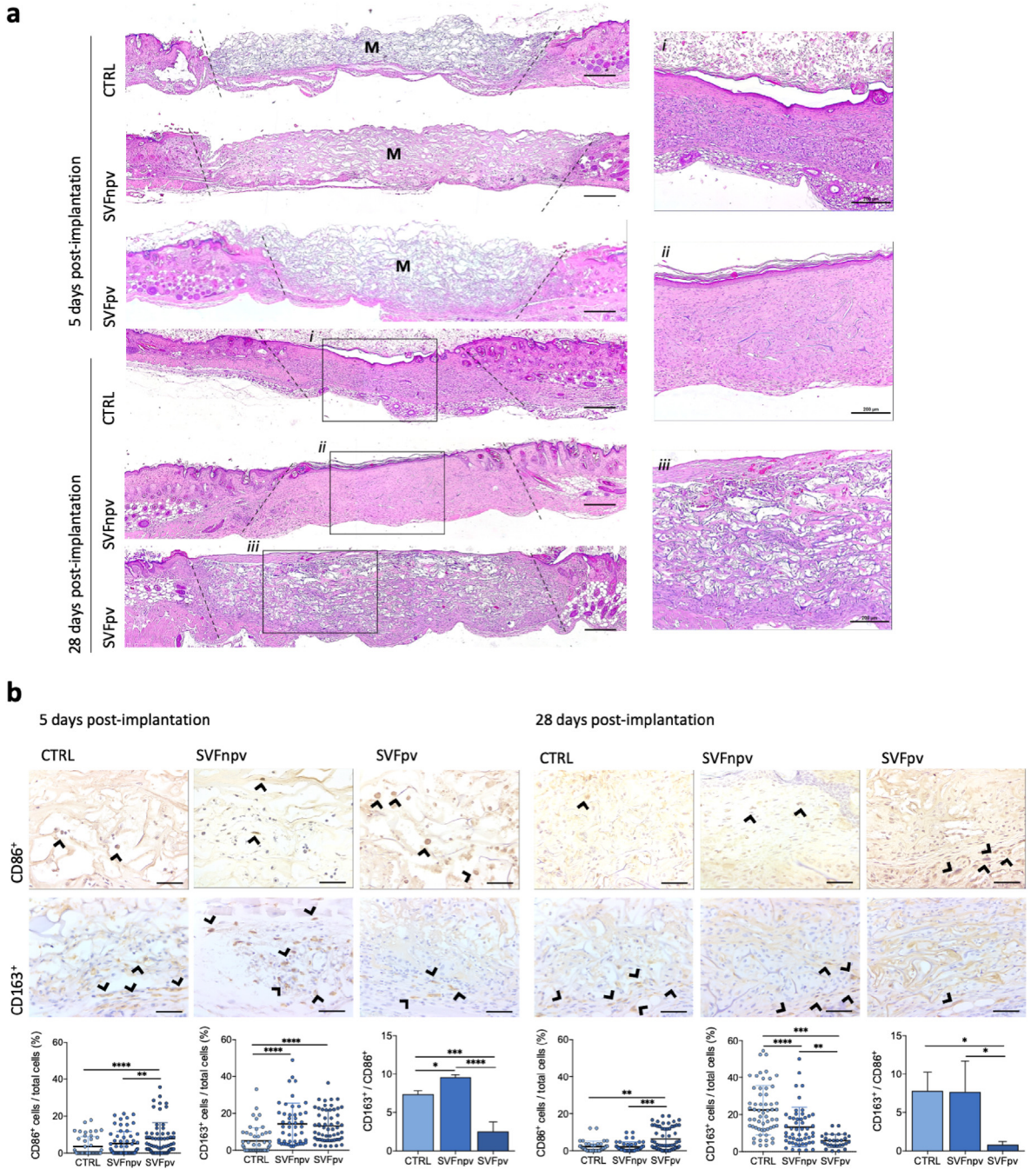

Fig. 4. Progression of the inflammatory process. a Representative images of haematoxylin and eosin (H&E) staining 5- and 28-days post-implantation. Scale bar = 1 mm. (i-iii) Higher magnification images of the area limited by the boxes in the lower magnification ones. Scale bar = 200 μm **b** Macrophage's recruitment and polarization 5- and 28-days post-transplantation. Representative immunostaining images of CD86 and CD163 (arrow heads) and quantification of the of $CD86^+$, $CD163^+$ cells and respective ratio. Scale bar = 50 μm. Quantitative results are expressed as the mean ± standard deviation where n = 3, * $p < 0.05$, ** $p < 0.01$, *** $p < 0.001$, **** $p < 0.0001$, one-way ANOVA with Tukey multiple comparison post-test. ———— wound margins; M – material.

pre-vascularization in vitro benefits the engraftment of the constructs indicating that this strategy can be an alternative to other similar strategies that rely on cells with limited availability.

Importantly, SVF is composed by a myriad of cells, including ASCs, that have been associated to biological processes with high relevance in cutaneous wound healing [20–22]. In this work, when SVF cells were cultured in the integrin-specific spongy-like hydrogels, despite the predominance of a vasculogenic phenotype [37] - progenitor $CD34^+$ and mature $CD31^+$ endothelial, and $CD146^+$ pericytic cells, we also found a sub-population expressing mesenchymal-associated markers - $CD105^+$, $CD73^+$ and $CD90^+$ [38,39]. While it is difficult to quantify the subset of cells corresponding to the ASCs due to their shared markers (CD34, CD105 and CD146) with the remaining cells and the respective changes associated to the culture conditions [40–43], it seems that the level of expression of all those markers increased or is maintained with time. This suggests that the vasculogenic process previously studied is accompanied by an enrichment of the mesenchymal population. Moreover, it appears that the mesenchymal population is supporting the vasculogenic cells to organize in capillary-like structures. This is in agreement with other works that showed the role of ASCs goes beyond modulation of mature endothelial cell migration through paracrine interactions [44] and capillary-like structure stabilization assuming a pericytic-like phenotype

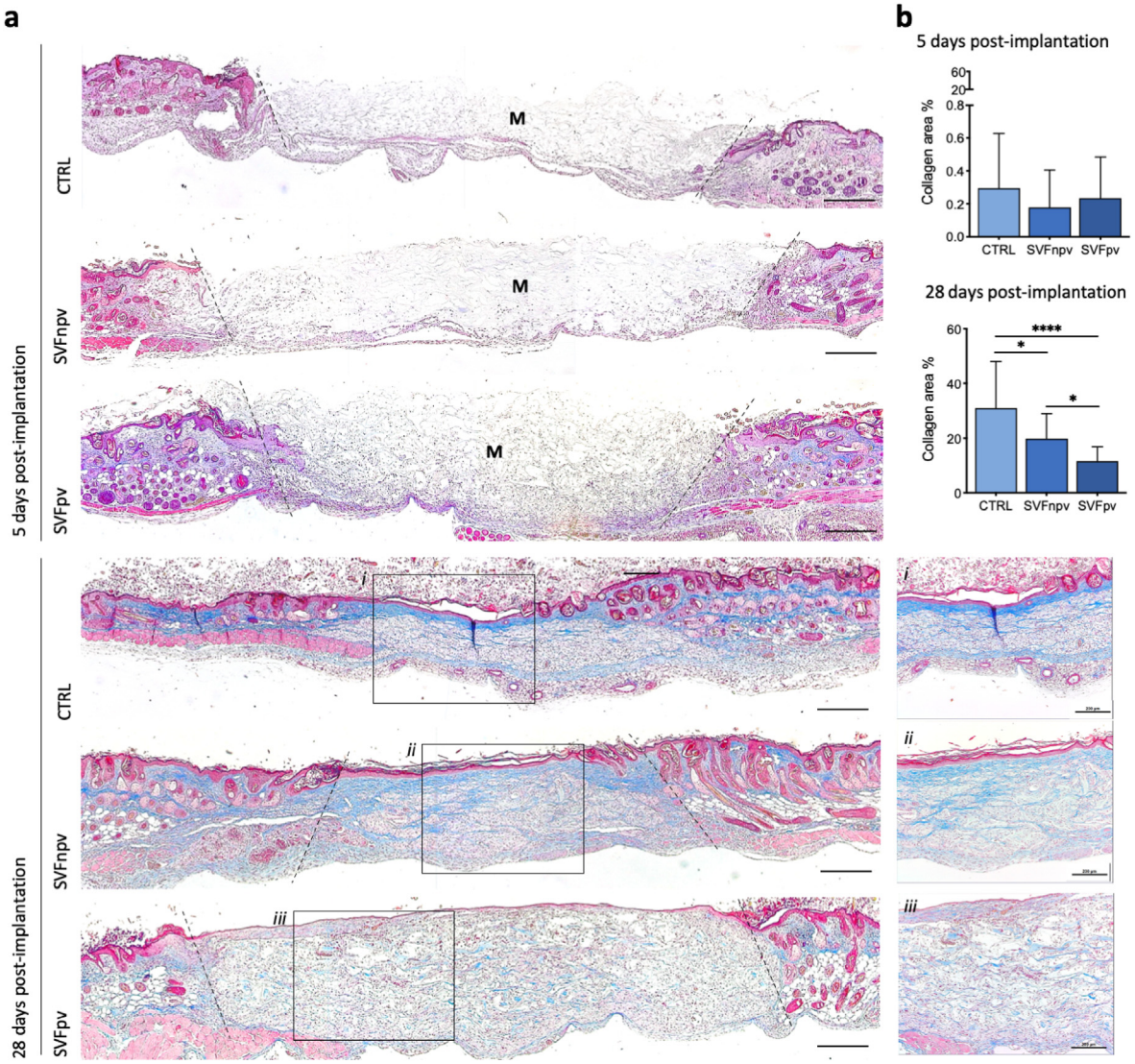

Fig. 5. Extracellular matrix deposition. a Representative images of Masson's Trichrome (MT) staining 5- and 28-days post-implantation. Scale bar = 1 mm. (i-iii) Higher magnification images of the area limited by the boxes in the lower magnification ones. Scale bar = 200 μm **b** Quantification of collagen relative to total area. Quantitative results are expressed as the mean ± standard deviation where n = 3, * $p < 0.05$, **** $p < 0.0001$, one-way ANOVA with Tukey multiple comparison post-test. ———— wound margins, M – material.

[42]. In fact, the potential of ASCs to stimulate vasculature morphogenesis has been also attributed to the fibronectin, laminin, perlecan-1 rich ECM produced by ASCs [45], some of the proteins that we found lining the prevascular network formed in our constructs.

Several works have suggested that the impact of SVF in cutaneous wounds goes beyond neovascularization, with both pre-clinical and clinical studies showing faster healing progression affecting re-epithelialization, inflammation and ECM deposition [28–30,46]. In agreement, we demonstrated that freshly isolated SVF incorporated in the spongy-like hydrogels foster re-epithelization leading to an epidermis with a higher degree of differentiation than the control condition. Moreover, we also confirmed the ability of the SVF to accelerate the resolution of the inflammatory phase as shown by the faster decay of proinflammatory M1 ($CD86^+$) macrophages and maintenance of the anti-inflammatory M2 ($CD163^+$) subtype. While the associated mechanism of action of the SVF is not well understood, it might be linked to the ASCs subpopulation that acts as homeostatic regulator of inflammation [24,25,46]. Moreover, as ASCs are entrapped within the integrin-specific biomaterials, their potential modulator secretome, including inflammatory mediators, such as interleukin (IL)-6, IL-10, granulocyte macrophage colony-stimulating factor, prostaglandin E2 and arginase-1 that are known to play a role in the M1 to M2 switch [24,25,47], might be maximized. However, a deeper understanding of this potential communication with macrophages and the exact mechanism behind M1 toM2 switch is still required.

According to previous works [48–52], prevascular networks that lead to improved anastomosis with the host blood vessels after transplantation, promote neotissue formation in cutaneous wound healing. Successful inosculation involves vascular remodeling of the readily perfusable networks with the host vessels [52]. While this process results in infiltration of inflammatory cells to the wound bed, it ensures the supply of nutrients and oxygen and the filling of the wound with a granulation tissue through which keratinocytes can migrate and re-epithelialize the wound. Our results showed that wound closure was slower in the prevascularized group than in the non-prevascularized, resulting in a lower degree of epidermal morphogenesis. We believe that this delayed re-epithelization in the prevascularized constructs might be related with the inflammatory phase of the wound healing process, as we detected

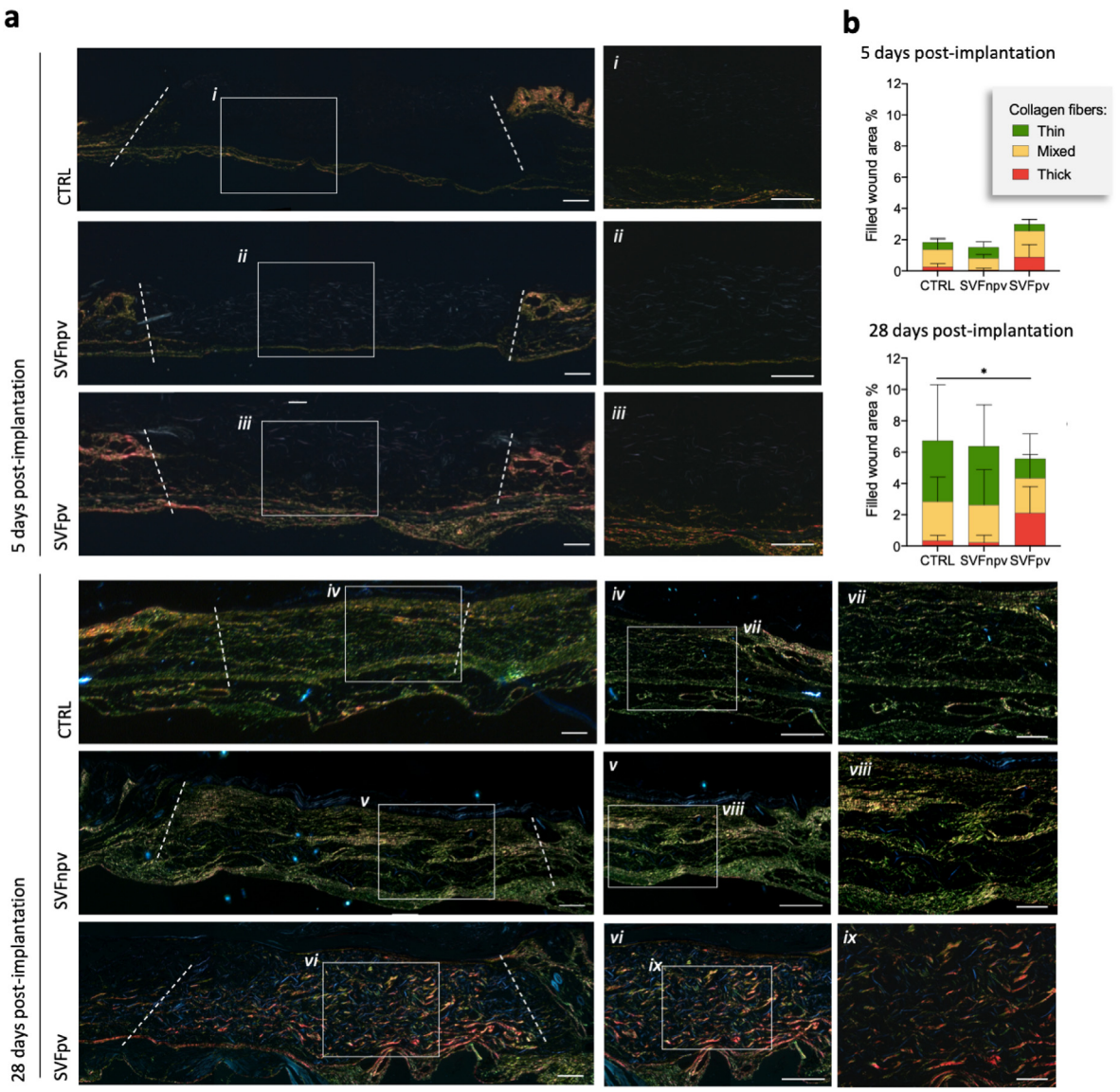

Fig. 6. Nature of deposited collagen. a Representative images of Picrosirius red staining of the wound site at day 5 and 28 post-implantation showing thick (red), mixed (yellow) and thin (green) collagen fibers. Scale bar = 500 μm. (i-ix) Higher magnification images of the area limited by the boxes in the lower magnification ones. Scale bar = 200 μm **b** Percentage of the wounded area filled with different types of collagen fibers (see Supplementary Fig. 1 for all individual comparisons). Quantitative results are expressed as the mean ± standard deviation where n = 3, * $p < 0.05$, one-way ANOVA with Tukey multiple comparison post-test. ———— wound margins.

significantly stronger response characterized by a higher percentage of M1 pro-inflammatory macrophages in this condition. The inosculation of the pre-formed vessels in our constructs with the host vessels seems to have facilitated the infiltration of inflammatory cells into the integrin-specific spongy-like hydrogels. Moreover, the low M2/M1 macrophages ratio observed in the prevascularized materials group, due to the persistence of $CD86^{+}$ macrophages along the time, is indicative of persistent inflammation. During the healing process, the transition from the inflammatory to the proliferative phase represents a key step towards wound closure [35]. The less-differentiated neodermis composed of a lower collagen density with thick collagen fibers in the prevascularized materials group further suggests that the healing process is not progressing. This also resulted in a delayed degradation of the material, in opposition to what was observed for the non-prevascularized construct that follows a sustained progression in the degradation of the material as well as the healing, in agreement with what was previously reported by us [46,53,54].

Based on our results, it can be assumed that the prevascularized system is not desired for cutaneous wound healing in which fast re-epithelialization is mandatory such as in the case of life-threatening extensive burns. Burn injuries lead to pathological scarring which is accompanied by aesthetic and functional sequelae thus, the quality of the healed tissue after a burn is also of outmost importance. We have previously shown that temporal modulation of the inflammatory stage in the healing of full-thickness wounds in diabetic mice impacts the quality of the neoskin formed suggesting that a slower, yet controlled, inflammation might be beneficial to that end [46]. Therefore, in less extensive burns in which the restoration of the external skin barrier is not the most immediate requirement, the prevascularized system might contribute to reduce the level of pathological scarring by modulating the healing temporal profile. In what concerns chronic wounds, since these are characterized by delayed re-epithelialization, it would be also reasonable to consider that while the prevascularized system would not be beneficial for these types of wounds, the system containing SVF cells

(non-prevascularized) would help to achieve fast wound closure with formation of the neodermis with adequate properties (collagen synthesis). Yet, delayed healing of chronic wounds is determined by a deficient angiogenic response therefore, from a vascularization point of view, the fast engraftment of the prevascularized system after anastomosis with the host vessels might allow overcoming the need for that priming of host angiogenesis. It is although evident that using a completely growth factor-free strategy that capable of improving wound neovascularization represents a very promising prospect for acute wounds.

Overall, we provide evidence that triggering vasculogenesis in vitro benefits neovascularization that also potentiates inflammatory cell influx, which negatively impact the progression of the cutaneous wound healing cascade. Despite this, the ability of SVF in non-prevascularized integrin-specific biomaterials in promoting an effective wound healing was guaranteed indicating that the proposed strategy can have enhanced efficacy.

4. Materials and methods

4.1. Gellan gum-based spongy-like hydrogels fabrication

Gellan gum was modified with vinyl sulfone moieties (DVS) as previously described [55]. Briefly, gelzan powder (0.25% w/v, Sigma, USA) was dissolved in deionized water (DI) at 90 °C. After dissolution, the pH was adjusted to 12 and DVS (Sigma, USA) was added in excess (molar ratio of 30:1) and left to react for 1 h. Gellan gum-divinyl sulfone (GGDVS) was purified by precipitation in cold diethyl ether (1:5) and dialysis against DI water for 3 days at 37 °C. The purified GGDVS was freeze-dried for further use. GG/GGDVS-RGD spongy-like hydrogels were prepared similarly to GG spongy-like hydrogels [55,56] with modifications. GGDVS was dissolved in ultra-pure (UP) water (pH 8) at RT. A solution of GGDVS-peptide (0.25% w/v with 800 μM of peptide) was prepared by letting the thiol-cyclo-RGD peptide (RGD, Cyclo (-RGDfC), >95% purity, GeneCust Europe) and GGDVS react for 1 h at RT under agitation. Meanwhile, a GG (0.5% w/v) solution was prepared as described above and allowed to reach 40 °C before mixing with the GGDVS-RGD solution. The solution (400 μM peptide) was cast into desired molds to form the hydrogels which were then frozen at −80 °C overnight and freeze-dried (Telstar, Spain) for 24 h to obtain the GG/GGDVS-peptide(s) dried polymeric networks. Spongy-like hydrogels were formed after rehydration of the dried polymeric networks with the cell suspension.

4.2. SVF isolation

Adipose tissue was harvested from fat tissue from skin specimens of healthy donors (IMC 20.8–26.8) undergoing abdominoplasties after written informed consent and under the protocol established and approved between the Ethical Committee of Hospital S. João (Porto, Portugal) (Nr 477/2020) and the Comissão de Ética para a Investigação em Ciências da Vida e da Saúde (CEICVS) (Nr 135/2020). Adipose tissue was digested with Collagenase type II (0.05% w/v, Sigma, USA) under agitation for 45 min at 37 °C. SVF was obtained after filtration and centrifugation (800 g, 10 min, 4 °C). SVF pellet was re-suspended in red blood cell lysis buffer (155 mM of ammonium chloride, 12 mM of potassium bicarbonate and 0.1 mM of ethylenediaminetetraacetic acid (EDTA), all from Sigma-Aldrich, Germany) and incubated for 10 min at RT. After centrifugation (300 g, 5 min, RT), the supernatant was discarded, and the cell pellet was re-suspended for immediate use.

4.3. Cell-laden GG/GGDVS-peptide(s) spongy-like hydrogels preparation

A SVF cell suspension containing 1.5×10^6 cells was prepared in Minimal Essential Medium (30 μL, α-MEM, Invitrogen, USA) supplemented with fetal bovine serum (10% v/v, FBS, Invitrogen, USA) and antibiotic/antimycotic solution (1% v/v, Invitrogen, USA) and dispensed dropwise on the top of the dried polymeric networks. Constructs were incubated for 30 min, at 37 °C, 5% CO_2 to allow maximum cell entrapment within the structures and then fresh medium was added.

4.4. Flow cytometry

Flow cytometry was conducted right after cell isolation and after 3 and 7 days of culture in the spongy-like hydrogels. After culture, cells were tripsinized from the spongy-like hydrogels using TrypLE™ Express Enzyme (Gibco, USA) for 15 min at 37 °C, 5% CO_2. The obtained cell suspension was filtered and centrifuged (5 min, 300 g, RT). Cells were incubated with CD105, CD73, CD90, CD45, CD34, CD31 and CD146 (Supplementary Table 1) antibodies for 20 min at RT at the concentrations advised by the manufacturer's, washed with PBS and resuspended in PBS with formalin (1% v/v, Bio-Optica, Italy). Cells were also labelled with DRAQ5 (eBioscience, USA) for nuclear staining to discern the cells of interest from the any remaining erythrocytes or tissue debris. 2×10^4 events were acquired in a BD FACSCalibur and analyzed using the Cyflogic version1.2.1 software.

4.5. Viability and cytoskeleton staining

Cell-laden spongy-like hydrogels were incubated with calcein-AM (Ca-AM, 1 μg mL^{-1}, Invitrogen, USA) and propidium iodide (PI, 2 μg mL^{-1}, Invitrogen, USA) for 1 h at 37 °C in a humidified incubator with 5% CO_2 atmosphere. For visualization of the cytoskeleton F-actin fibers and nuclei, cells were fixed with formalin (10% v/v) for 1 h at RT, and stained with phalloidin-TRITC (0.1 mg mL^{-1}, Sigma, USA) and DAPI (0.02 mg mL^{-1}) for 2 h at RT. Both cell viability and cytoskeleton organization were observed with a Leica TCS SP8 confocal microscope (Leica, Germany).

4.6. Immunocytochemistry

Cell-laden spongy-like hydrogels were fixed with formalin (10% v/v) for 24 h at RT and then incubated with Triton X-100 (0.2% v/v, Sigma-Aldrich, Portugal) for 30 min at RT for cell permeabilization. Afterwards, samples were blocked with bovine serum albumin (BSA, 3% w/v, Sigma-Aldrich, Portugal) for 1 h and then incubated with anti-human primary antibodies (Supplementary Table 2) diluted in BSA (1% w/v) solution in PBS overnight at 4 °C. After washing with PBS, samples were incubated 1 h at RT with the secondary antibody Alexa Fluor 488 donkey anti-mouse (1:500, Life Technologies, CA, USA) in BSA (1% w/v) solution in PBS. Nuclei were counter-stained with DAPI. Constructs were observed using a Leica TCS SP8 confocal microscope (Leica, Germany).

4.7. In vivo assay

The experiment was approved by the Direcção Geral de Alimentação Veterinária (DGAV), the Portuguese National Authority for Animal Health, and all the surgical procedures respected the national regulations and the international animal welfare rules, according to the Directive 2010/63/EU. Athymic nude mice NU(NCr)-Foxn1nu (Charles River, France) with 6 weeks old were randomly assigned to 3 groups: (i) GG/GGDVS-RGD spongy-like hydrogels – control; (ii) GG/GGDVS-RGD spongy-like hydrogels with freshly isolated SVF cells – SVFnpv; (iii) GG/GGDVS-RGD spongy-like hydrogels cultured for 7 days with SVF cells – SVFpv. A total of 54 animals, 6 animals per condition and per time point (5 and 28 days) were used. Mice were anaesthetized with an i. p injection of a mixture of ketamine (75 mg kg^{-1}, Imalgene, Merial, France) and metedomidine (1 mg kg^{-1}, Domitor, Orion Pharma, Finland). The back of the animals was disinfected with betaisodone and 70% ethanol. A 5 mm ∅ skin full-thickness excision was created and a donut-shaped 5 mm silicone splint (ATOS Medical, Sweden) was glued and sutured around the wound to minimize wound contraction. After transplantation of the constructs, wounds were successively covered with

Tegaderm transparent dressing (3 M, USA), Omnifix (Hartmann, USA) and Leukoplast (Essity, Spain). After surgery, atipamezole (1 mg kg^{-1}, Antisedan, Pfizer, Finland) was administered to the animals. The animals were kept separately and received daily analgesia with metamizole (200 μg g^{-1} BW, Nolotil, Boehringer Ingelheim, Germany) in the drinking water for the first 72 h. At each time-point the assigned animals were sacrificed by CO_2 inhalation and the constructs/tissue were explanted for histological analysis.

4.8. Wound closure quantification

Wound closure was calculated according to Equation 1, by analyzing the wound area in the digital images taken at the time of material implantation (A) and 5, 11 and 28 days post-implantation (B) in five animals per condition and time-point.

Wound closure (%) = [(A - B)/A] x 100 (1).

4.9. Histological analysis

Explanted tissue was fixed in formalin (10% v/v), dehydrated, embedded in paraffin (Thermo Scientific, USA) and cut into 4.5 μm sections. Tissue sections were stained with Haematoxylin & Eosin (Sigma, USA), Masson's Trichrome kit (Bio-Optica, Italy) and Picrosirius Red kit (Bio-Optica, Italy) following routine protocols. For immunohistochemistry, paraffin tissue sections were deparaffinized in xylene, rehydrated and boiled for 5 min in Tris-EDTA buffer (10 m M Tris Base, 1 mM EDTA solution and, 0.05% v/v Tween 20, pH 9) for antigen retrieval. Afterwards, permeabilization was carried out with Triton X-100 (0.2% v/v) and unspecific staining was blocked with Horse Serum (2.5%, Vector Labs, CA, USA). Primary antibodies (Supplementary Table 2) were incubated overnight at 4 °C. For detection, VECTASTAIN Elite ABC Kit (Vector Labs) was used according to the manufacturer's instructions. Nuclei were stained with Gill's haematoxylin. All samples were examined under a Leica DM750 microscope, using LEICA Acquire software.

4.10. Image analysis

Five images of random fields were acquired for each condition and experiment and used to calculate the number of cells (DAPI stained) with the Cell Profiler software.

To infer about the number of CD163 and CD86 positive cells, six images of random fields of four non-consecutive tissue sections per time-point and per animal were used with the Cell Profiler software using an algorithm for the identification of nuclei (haematoxylin)-associated DAB staining. Results are presented as positive cells per total cell amount. Ratio of the CD163 positive cells per CD86 positive cells ($CD163^{+}$/$CD86^{+}$) was calculated from the average values of positive cells for each animal. From the Masson's Trichrome stained sections, a custom-written algorithm was used to identify the blue pixels (collagen) keeping the same color segmentation settings for each image. The amount of collagen was calculated as percentage of total pixels. The same algorithm was used to identify the different color pixels from the Picrosirius Red stained sections - green pixels were considered thin, yellow pixels were considered mixed, and red pixels were considered thick fibers [57]. The respective type of collagen fibers was calculated as percentage of total pixels.

Neoepidermis thickness at the end-point was measured at the wounded area, considering the basal epidermis layer up to the outermost layer of nucleated cells.

4.11. Statistical analysis

Statistical analysis was performed using the PRISM software, version 8.2.1 for Mac OS X or Windows (GraphPad Software Inc., San Diego, USA). Shapiro–Wilk test was performed to validate normality of data prior to statistical testing and all data followed a normal distribution. Therefore, the one-way or two-way analysis of variance (ANOVA) with a Tukey multiple comparison post-test was used to analyze the results. Significance was set to 0.05 (95% of confidence interval). All quantitative data refer to 3 independent experiments (n = 3) with at least 3 replicates in each condition in each experiment and are presented as mean ± standard deviation.

Author contributions

H.R.M., R.P.P. and A.P.M contributed to the conceptual design of the original project, designed experiments, analysis and validation of the data, and participated in the figure design. H.R.M. contributed with the experimental execution. D.B.R. and R.P.P. contributed to experimental execution and troubleshooting for *in vivo* experiments, and analysed in vivo data. A.d.S.M. contributed to experimental execution of the *in vivo* experiment. S.F.R. contributed to isolation and characterization of SVF cells provided by M.J. and R.H.. L.P.d.S. contributed to experimental preparation of the materials used in the manuscript. While the original draft preparation was done by H.R.M., review and editing were performed by R.P.P. and A.P.M. R.L.R. and A.P.M. contributed with supervision, project administration and funding acquisition. All authors have read and agree to the published version of the manuscript.

Declaration of competing interest

The authors declare that they have no known competing financial interests or personal relationships that could have appeared to influence the work reported in this paper.

Data availability

Data will be made available on request.

Acknowledgments

Authors would like to acknowledge the financial support from the Consolidator Grant “ECM_INK” (ERC-2016-COG-726061) and the Starting Grant “CapBed” (ERC-2018-STG-805411), to the FSE/POCH (Fundo Social Europeu através do Programa Operacional do Capital Humano) under the scope of the PD/169/2013, NORTE-08-5369-FSE-000037 (H.R.M.), and to FCT/MCTES (Fundação para a Ciência e a Tecnologia/Ministério da Ciência, Tecnologia, e Ensino Superior) through the grants SFRH/BD/119756/2016 (D.B.R.), PhD grant PD/BD/135252/2017 (S.F.R.) and IF/00347/2015 (R.P.P.). Authors would also like to acknowledge BioRender.com as a platform for image creation.

Appendix A. Supplementary data

Supplementary data to this article can be found online at https://doi.org/10.1016/j.mtbio.2022.100496.

References

[1] M.G. Tonnesen, X. Feng, R.A.F. Clark, J. Invest. Dermatol. Symp. Proc. 5 (2000) 40.
[2] R.J. Bodnar, Adv. Wound Care 4 (2015) 641.
[3] A. Vijayan, S. A, G.S.V. Kumar, Sci. Rep. 9 (2019), 19165.
[4] G. Long, D. Liu, X. He, Y. Shen, Y. Zhao, X. Hou, B. Chen, W. OuYang, J. Dai, X. Li, Biomater. Sci. 8 (2020) 6337.
[5] Y. Qu, C. Cao, Q. Wu, A. Huang, Y. Song, H. Li, Y. Zuo, C. Chu, J. Li, Y. Man, J. Tissue Eng. Regen. Med. 12 (2018) 1508.
[6] J. Ishihara, A. Ishihara, K. Fukunaga, K. Sasaki, M.J.V. White, P.S. Briquez, J.A. Hubbell, Nat. Commun. 9 (2018) 2163.
[7] D. Lou, Y. Luo, Q. Pang, W.Q. Tan, L. Ma, Bioact. Mater. 5 (2020) 667.
[8] P. Wang, S. Huang, Z. Hu, W. Yang, Y. Lan, J. Zhu, A. Hancharou, R. Guo, B. Tang, Acta Biomater. 100 (2019) 191.
[9] M.T. Cerqueira, R.P. Pirraco, T.C. Santos, D.B. Rodrigues, A.M. Frias, A.R. Martins, R.L. Reis, A.P. Marques, Biomacromolecules 14 (2013) 3997.

[10] O. Fujiwara, A. Prasai, D. Perez-Bello, A. El Ayadi, I. Petrov, R. Esenaliev, Y. Petrov, D. Herndon, C. Finnerty, D. Prough, et al., Burn. trauma 8 (2020), tkaa009.
[11] H. Nagano, Y. Suematsu, M. Takuma, S. Aoki, A. Satoh, E. Takayama, M. Kinoshita, Y. Morimoto, S. Takeoka, T. Fujie, et al., Sci. Rep. 11 (2021), 14500.
[12] D.M. Burmeister, R. Stone, , II, N. Wrice, A. Laborde, S.C. Becerra, S. Natesan, R.J. Christy, Stem Cells Transl. Med. 7 (2018) 360.
[13] N. Ebrahim, A.A. Dessouky, O. Mostafa, A. Hassouna, M.M. Yousef, Y. Seleem, E.A.E.A.M. El Gebaly, M.M. Allam, A.S. Farid, B.A. Saffaf, et al., Stem Cell Res. Ther. 12 (2021) 392.
[14] I. Montaño, C. Schiestl, J. Schneider, L. Pontiggia, J. Luginbühl, T. Biedermann, S. Böttcher-Haberzeth, E. Braziulis, M. Meuli, E. Reichmann, Tissue Eng. 16 (2010) 269.
[15] M.T. Cerqueira, R.P. Pirraco, a.R. Martins, T.C. Santos, R.L. Reis, a.P. Marques, Acta Biomater. 10 (2014) 3145.
[16] T. Sasagawa, T. Shimizu, M. Yamato, T. Okano, J. Tissue Eng. Regen. Med. 10 (2016) 739.
[17] T. Baltazar, J. Merola, C. Catarino, C.B. Xie, N.C. Kirkiles-Smith, V. Lee, S. Hotta, G. Dai, X. Xu, F.C. Ferreira, et al., Tissue Eng. 26 (2020) 227.
[18] R.M. Raftery, E.G. Tierney, C.M. Curtin, S.-A.A. Cryan, F.J. O'Brien, J. Contr. Release 210 (2015) 84.
[19] R.J. Medina, C.L. O'Neill, T.M. O'Doherty, S.E.J. Chambers, J. Guduric-Fuchs, J. Neisen, D.J. Waugh, D.A. Simpson, A.W. Stitt, Stem Cell. 31 (2013) 1657.
[20] A.J. Melchiorri, B.N.B. Nguyen, J.P. Fisher, Tissue Eng. B Rev. 20 (2014) 218.
[21] M.W. Laschke, S. Kleer, C. Scheuer, S. Schuler, P. Garcia, D. Eglin, M. Alini, M.D. Menger, Eur. Cell. Mater. 24 (2012) 266.
[22] J. Rehman, D. Traktuev, J. Li, S. Merfeld-Clauss, C.J. Temm-Grove, J.E. Bovenkerk, C.L. Pell, B.H. Johnstone, R.V. Considine, K.L. March, Circulation 109 (2004) 1292.
[23] M. Moriyama, S. Sahara, K. Zaiki, A. Ueno, K. Nakaoji, K. Hamada, T. Ozawa, D. Tsuruta, T. Hayakawa, H. Moriyama, Sci. Rep. 9 (2019), https://doi.org/10.1038/s41598-019-54797-5.
[24] H.D. Zomer, T. da S. Jeremias, B. Ratner, A.G. Trentin, Cytotherapy (2020) 22, https://doi.org/10.1016/j.jcyt.2020.02.003.
[25] J. Wang, H. Hao, H. Huang, D. Chen, Y. Han, W. Han, BioMed Res. Int. (2016) 2016, https://doi.org/10.1155/2016/1464725.
[26] V. Planat-Benard, J.-S. Silvestre, B. Cousin, M. André, M. Nibbelink, R. Tamarat, M. Clergue, C. Manneville, C. Saillan-Barreau, M. Duriez, et al., Circulation 109 (2004) 656.
[27] K. Yoshimura, T. Shigeura, D. Matsumoto, T. Sato, Y. Takaki, E. Aiba-Kojima, K. Sato, K. Inoue, T. Nagase, I. Koshima, et al., J. Cell. Physiol. 208 (2006) 64.
[28] M.H. Carstens, F.J. Quintana, S.T. Calderwood, J.P. Sevilla, A.B. Ríos, C.M. Rivera, D.W. Calero, M.L. Zelaya, N. Garcia, K.A. Bertram, et al., Stem Cells Transl. Med. (2021) 10, https://doi.org/10.1002/sctm.20-0497.
[29] M.A. Nilforoushzadeh, M.M. Sisakht, M.A. Amirkhani, A.M. Seifalian, H.R. Banafshe, J. Verdi, M. Nouradini, J. Tissue Eng. Regen. Med. 14 (2020) 424.
[30] S. Atalay, A. Coruh, K. Deniz, Burns (2014) 40, https://doi.org/10.1016/j.burns.2014.01.023.
[31] H.R. Moreira, D.B. Rodrigues, S. Freitas-Ribeiro, L.P. da Silva, A. da S. Morais, M. Jarnalo, R. Horta, R.L. Reis, R.P. Pirraco, A.P. Marques, npj Regen. Med. 7 (2022) 57.
[32] S.M. Weis, D.A. Cheresh, Cold Spring Harb. Perspect. Med. 1 (2011) a006478.
[33] R. Silva, G. D'Amico, K.M. Hodivala-Dilke, L.E. Reynolds, Arterioscler. Thromb. Vasc. Biol. 28 (2008) 1703.
[34] L.A. DiPietro, J. Leukoc. Biol. 100 (2016) 979.
[35] N.X. Landén, D. Li, M. Ståhle, Cell. Mol. Life Sci. 73 (2016) 3861.
[36] S.A. Eming, P. Martin, M. Tomic-Canic, Sci. Transl. Med. 6 (2014), https://doi.org/10.1126/scitranslmed.3009337.
[37] A. Miranville, C. Heeschen, C. Sengenès, C.A. Curat, R. Busse, A. Bouloumié, Circulation 110 (2004), https://doi.org/10.1161/01.CIR.0000135466.16823.D0.
[38] J.B. Mitchell, K. McIntosh, S. Zvonic, S. Garrett, Z.E. Floyd, A. Kloster, Y. Di Halvorsen, R.W. Storms, B. Goh, G. Kilroy, et al., Stem Cell. 24 (2006), https://doi.org/10.1634/stemcells.2005-0234.
[39] M. Costa, M.T. Cerqueira, T.C. Santos, B. Sampaio-Marques, P. Ludovico, A.P. Marques, R.P. Pirraco, R.L. Reis, Acta Biomater. 55 (2017) 131.
[40] Q. Peng, H. Alipour, S. Porsborg, T. Fink, V. Zachar, Int. J. Mol. Sci. 21 (2020), https://doi.org/10.3390/ijms21041408.
[41] M. Dominici, K. Le Blanc, I. Mueller, I. Slaper-Cortenbach, F.C. Marini, D.S. Krause, R.J. Deans, A. Keating, D.J. Prockop, E.M. Horwitz, Cytotherapy 8 (2006), https://doi.org/10.1080/14653240600855905.
[42] A.S. Klar, S. Güven, J. Zimoch, N.A. Zapiórkowska, T. Biedermann, S. Böttcher-Haberzeth, C. Meuli-Simmen, I. Martin, A. Scherberich, E. Reichmann, et al., Pediatr. Surg. Int. 32 (2016) 17.
[43] H. Suga, D. Matsumoto, H. Eto, K. Inoue, N. Aoi, H. Kato, J. Araki, K. Yoshimura, Stem Cell. Dev. 18 (2009), https://doi.org/10.1089/scd.2009.0003.
[44] F.M. Nielsen, S.E. Riis, J.I. Andersen, R. Lesage, T. Fink, C.P. Pennisi, V. Zachar, Stem Cell Res. Ther. 7 (2016), https://doi.org/10.1186/s13287-016-0435-8.
[45] S. Merfeld-Clauss, N. Gollahalli, K.L. March, D.O. Traktuev, Tissue Eng. 16 (2010), https://doi.org/10.1089/ten.tea.2009.0635.
[46] L.P. da Silva, T.C. Santos, D.B. Rodrigues, R.P. Pirraco, M.T. Cerqueira, R.L. Reis, V.M. Correlo, A.P. Marques, J. Invest. Dermatol. 137 (2017) 1541.
[47] J.D. Glenn, World J. Stem Cell. 6 (2014), https://doi.org/10.4252/wjsc.v6.i5.526.
[48] D. Chouhan, N. Dey, N. Bhardwaj, B.B. Mandal, Biomaterials 216 (2019), 119267.
[49] L. Gibot, T. Galbraith, J. Huot, F.A. Auger, Tissue Eng. 16 (2010), https://doi.org/10.1089/ten.tea.2010.0189.
[50] H. Miyazaki, Y. Tsunoi, T. Akagi, S. Sato, M. Akashi, D. Saitoh, Sci. Rep. 9 (2019), https://doi.org/10.1038/s41598-019-44113-6.
[51] S.B. Riemenschneider, D.J. Mattia, J.S. Wendel, J.A. Schaefer, L. Ye, P.A. Guzman, R.T. Tranquillo, Biomaterials 97 (2016) 51.
[52] M.W. Laschke, B. Vollmar, M.D. Menger, Tissue Eng. B Rev. 15 (2009) 455.
[53] M.T. Cerqueira, L.P. Da Silva, T.C. Santos, R.P. Pirraco, V.M. Correlo, A.P. Marques, R.L. Reis, Tissue Eng. 20 (2014) 1369.
[54] M.T. Cerqueira, L.P. Da Silva, T.C. Santos, R.P. Pirraco, V.M. Correlo, R.L. Reis, A.P. Marques, ACS Appl. Mater. Interfaces 6 (2014), 19668.
[55] L.P. da Silva, A.K. Jha, V.M. Correlo, A.P. Marques, R.L. Reis, K.E. Healy, Adv. Healthc. Mater. 7 (2018), 1700686.
[56] H.R. Moreira, L.P. da Silva, R.L. Reis, A.P. Marques, Polymers 12 (2020) 329.
[57] C.R. Drifka, A.G. Loeffler, K. Mathewson, G. Mehta, A. Keikhosravi, Y. Liu, S. Lemancik, W.A. Ricke, S.M. Weber, W.J. Kao, et al., J. Histochem. Cytochem. 64 (2016), https://doi.org/10.1369/0022155416659249.